Journal of Bioresources and Bioproducts 8 (2023) 224–234

Contents lists available at ScienceDirect

Journal of Bioresources and Bioproducts

journal homepage: https://www.keaipublishing.com/en/journals/journal-of-bioresources-and-bioproducts/

Research Article

Preparation and characterization of tea tree oil-β-cyclodextrin microcapsules with super-high encapsulation efficiency

Peifu Kong[a], Junichi Peter Abe[b], Shunsuke Masuo[b], Toshiharu Enomae[b,*]

[a] Degree Programs in Life and Earth Sciences, University of Tsukuba, Ibaraki 305-8572, Japan
[b] Faculty of Life and Environmental Sciences, University of Tsukuba, Ibaraki, 305-8572, Japan

ARTICLE INFO

Keywords:
β-cyclodextrin
Co-precipitation
Encapsulation efficiency
Microcapsule
Tea tree oil

ABSTRACT

This study aimed to prepare tea tree oil-β-cyclodextrin microcapsules using an optimized co-precipitated method. The impact of the volume fraction of ethanol in the solvent system for microencapsulation on encapsulation efficiency was investigated and analyzed sophisticatedly. Super-high encapsulation efficiency was achieved when a 40% volume fraction of ethanol was used for the microencapsulation procedure, where the recovery yield of microcapsules and the embedding fraction of tea tree oil in microcapsules were as high as 88.3% and 94.3%, respectively. Additionally, considering the operation cost, including time and energy consumption, an economical preparation was validated so that it would be viable for large-scale production. Based on the results of morphological and X-ray diffraction analysis, the crystal structure appeared to differ before and after microencapsulation. The results of gas chromatography-mass spectrometry and Fourier transform infrared spectroscopy confirmed the successful formation of microcapsules. Furthermore, the antibacterial activity of the fabricated microcapsules was assessed by a simple growth inhibition test using *Bacillus subtilis* as the study object, and the hydrophilic property was proved by a water contact angle measurement.

1. Introduction

Essential oils (EOs) are a mixture of secondary metabolites of plants, which play an imperative role in the plant defense system and are mainly well known for their antimicrobial and antitumor activities (Mishra et al., 2020). In recent years, extensive interest towards some EOs (e.g., cinnamon, thyme, oregano, and clove oils) have fostered the advancement of the fields of food, medicine, agriculture, and cosmetics, since they have been generally recognized as safe additives by the U.S. Food and Drug Administration (Sadgrove and Jones, 2015; Sarkic and Stappen, 2018; Ju et al., 2019; Zhang and Yao, 2019). Especially in the field of food packaging, there has been considerable attention devoted to the utilization of EOs in conjunction with various hydrophilic biodegradable natural polymers (e.g., chitosan, cellulose, gelatin, and alginate) to obtain antimicrobial composite films or coatings because of the pressure of environmental concerns stemming from the traditional petroleum-based materials (Ju et al., 2019; Sharma et al., 2021). Tea tree oil (TTO), extracted from Australian native tree *Melaleuca alternifolia*, is almost colorless and hence appears to be preferable to apply as light-colored EOs for preventing the spoilage of visual effects on subsequent products. It has been revealed that TTO can effectively inhibit not only the growth of bacteria and viruses, but also that of molds and yeasts (Lam et al., 2020; Sathiyaseelan et al., 2021). Despite its advantages, TTO has not been widely employed on a large scale due to its high volatility, thermolability, and easy oxidation in undesirable environmental conditions, which impede its functional performance (Jiang et al., 2021b). Furthermore, its high hydrophobicity severely limits its compatibility with hydrophilic biodegradable polymers.

* Corresponding author.
E-mail address: toshiharu.fw@u.tsukuba.ac.jp (T. Enomae).

https://doi.org/10.1016/j.jobab.2023.03.004

Microencapsulation using β-cyclodextrin (β-CD) is a promising approach to prevent those performance reductions mentioned above and could achieve a superiority of prolonged-release as well (Aytac et al., 2016; Lis et al., 2018). Additionally, it is anticipated that microencapsulation might minimize the negative effect of TTO odor on the organoleptic quality of follow-up applications. Microencapsulation is a technique by which one material (core) is embedded within another material (wall) to form a microcapsule complex. The β-CD, recognized as a nontoxic and eco-friendly ingredient, is a truncated-cone-shaped cyclic oligosaccharide comprising seven glucose units (Fig. S1) (Astray et al., 2009). It has a hydrophilic outer surface and hydrophobic hollow cavity which can embed TTO by their similar physical property (Liu et al., 2021). Moreover, the hydrophilic nature of the outer surface allows it to integrate easier with hydrophilic biodegradable materials for versatile applications.

Co-precipitation is the most widely used microencapsulation technique, as well as the most practicable, owing to its ease of operation and prospective economic viability (Shrestha et al., 2017). However, the low encapsulation efficiency has become an intractable and primary barrier for large-scale applications and commercialization. Ma et al. (2018) optimized the encapsulation process of clove oil using a response surface methodology under different experimental conditions of temperature, time, and wall-to-core ratio. Ning and Yue (2019) also performed a similar optimization process of microencapsulation for eucalyptus oil by the response surface methodology; however, their encapsulation efficiencies (below 80%) remained at a low level. Therefore, some β-CD derivatives, such as hydroxypropyl-β-cyclodextrin, have been effective in drawing the attention of some researchers (Yao et al., 2014; Wei et al., 2017; Gao et al., 2021). Nevertheless, on the contrary, significant shortcomings of these derivatives, such as the threat of nephrotoxicity (Li et al., 2016), high cost, and low affinity for some bioactive components of EOs (de Almeida Magalhães et al., 2020), have been reported successively. Hence, the improvement of the encapsulation efficiency of β-CD has been desired.

Since the co-solvent system of water and ethanol with a volume ratio of 2 was introduced by Reineccius and Risch (1986), it has been perpetuated in use for the co-precipitation method (Wang et al., 2011; Abarca et al., 2016; Wen et al., 2016; Anaya-Castro et al., 2017; Kotronia et al., 2017; Herrera et al., 2019). It is reported that the hydrophobic cavity of β-CD is initially occupied by enthalpy-rich ethanol molecules in the co-solvent (Astray et al., 2009). After the addition of EOs, the primary driving force of microcapsule formation is the displacement of enthalpy-rich ethanol molecules by more hydrophobic EOs compounds, resulting in a more stable and lower-energy state (Abarca et al., 2016). Conceivably, the fraction of ethanol in the co-solvent may have a significant impact on the encapsulation efficiency. Importantly, no study has yet been conducted regarding this based on available resources. Therefore, the objective of this study was to: 1) microencapsulate TTO with β-CD, 2) investigate the impact of the volume fraction of ethanol in the co-solvent on encapsulation efficiency, and 3) elucidate the physicochemical characteristics of the fabricated microcapsules.

2. Materials and methods

2.1. Raw materials

The β-CD (Wako 1st Grade) and ethanol (99.5%, *V*, guaranteed reagent) were obtained from FUJIFILM Wako Chemicals, Japan. The TTO was bought from Salvia Cosmeceuticals Pvt. Ltd., India. Tryptic soy agar (TSA) was provided by Geno Technology Inc., USA. The *Bacillus subtilis*, ATCC 19659, were obtained from Microbiologics, Inc., USA.

2.2. Preparation of TTO-β-CD microcapsules

Microcapsules were produced according to a methodology described in our previous studies with some optimizations (Kong et al., 2022a, b). A total of 3 g β-CD was put in a beaker and dissolved in a 50 mL co-solvent of distilled water and ethanol (99.5%) and magnetically stirred at 700 r/min, with the temperature of 60 °C (± 2 °C) on a hot stirrer plate (RSH-6DN, AS ONE Corporation, Japan). A prior test has confirmed that only ~1.5 g β-CD could be successfully dissolved in a 50 mL water-solvent, and 3 g β-CD could not be completely soluble in a 50 mL co-solvent of distilled water and ethanol (99.5%) with a volume ratio of 1. Therefore, the volume fraction of ethanol in the co-solvent in this study was prepared as 25%, 29%, 33%, and 40%, corresponding to the volume ratio of distilled water to ethanol being 3.0, 2.5, 2.0, and 1.5. Then, the beaker was covered with aluminum foil. After cooling the co-solvent to 45 °C (± 2 °C), 0.33 g TTO was added swiftly using a syringe through a small hole when the aluminum foil was lifted slightly, and the hot stirrer plate was sheltered with a paper box to prevent TTO oxidation from illumination, followed by a constant magnetic stirring at 45 °C (± 2 °C) for 2 h and then maintained for 24 h at −2 °C (± 1 °C). The cold precipitate (supposed to be TTO-β-CD microcapsules) was recovered via a suction filtration (AS-01, AS ONE Corporation, Japan) with a filter paper with a pore diameter of 1 μm (No. 4, Kiriyama glass Co., Japan) and rinsed with 40 mL ethanol (60%, *V*) to remove the residual TTO on the surface. Finally, the TTO-β-CD microcapsules were dried in a desiccator at 23 °C for 24 h under the condition of non-illumination and hermetically stored in a brown glass bottle at 23 °C for subsequent characterization.

2.3. Determination of encapsulation efficiency

Recovery yield (R_Y) and TTO embedding fraction (E_F) were calculated using Eqs. (1) and (2), respectively, to assess the encapsulation efficiency of the microencapsulation procedure.

$$R_Y(\%) = \frac{\text{Total weight of recovered TTO-}\beta\text{-CD microcapsules}}{\text{Initial }\beta\text{-CD weight} + \text{Initial TTO weight}} \times 100\% \quad (1)$$

$$E_F(\%) = \frac{\text{Weight of embedded TTO}}{\text{Initial TTO weight}} \times 100\% \quad (2)$$

The weight of embedded TTO was determined via a method described in our previous study (Kong et al., 2022a) with some modifications. Briefly, a total of 0.50 g TTO was added to 50 mL ethanol (99.5%, *V*) (solution-1). Then, 0.5 mL solution-1 was adjusted to 50 mL with ethanol (99.5%) (solution-2). Finally, 1, 2, 3, 4, and 5 mL solution-2 were taken and diluted to 10 mL with ethanol (99.5%) to form five gradient standard samples, i.e., 0.01, 0.02, 0.03, 0.04, and 0.05 g/L. The absorbance at 264 nm (Fig. S2) of these standard samples was measured using a ultraviolet-visible (UV–visible) spectrophotometer (UV-3100 PC, Shimadzu, Japan). A calibration curve was drawn to exhibit the relationship between the concentration of TTO and the absorbance at 264 nm ($y = 2.488\ 5x + 0.000\ 8$, $R^2 = 0.999\ 5$, Fig. S3). A total of 0.04 g TTO-β-CD microcapsules were extracted with 40 mL ethanol (99.5%) in a 50 mL centrifuge tube (AS ONE Corporation, Japan) using a vortex mixer (HS120214, Heathrow Scientific, LLC, USA) at 3 000 r/min for 10 min, followed by a few steps of centrifugation at 1 700 g for 10 min and sedimentation in the dark at 23 °C for 12 h. After that, ~2 mL of supernatant was filtered using a syringe filter (Diameter: 25 mm, Membrane Solutions, USA) with a pore diameter of 0.22 μm. Finally, the absorbance at 264 nm of the filtrate was measured with the ethanol (99.5%) as the blank solution, and the content of TTO embedded in microcapsules was calculated by the calibration curve.

2.4. Physicochemical characterization of TTO-β-CD microcapsules

The morphological structure of the TTO-β-CD microcapsules was observed using a scanning electron microscope (SEM, TM4000Plus, Hitachi, Japan) in the backscattered electron mode at a low-vacuum condition to diminish volatilization of compounds embedded in the microcapsules. The microcapsules were coated with sputtered platinum for high conductivity before the observation and imaged at an accelerated voltage of 10 kV. As a control, the purchased plain β-CD was observed in the same condition.

The variation in crystal structure before and after the microencapsulation procedure was analyzed using an X-ray diffractometer (XRD, D8 ADVANCE/TSM, Bruker AXS, USA). The XRD patterns of plain β-CD and TTO-β-CD microcapsules were obtained using Cu-Kα radiation, at an accelerated voltage of 40 kV and a current of 40 mA. All scans were performed at the 2θ angle ranging from 2°–30° with an increment of 0.02°

The formation of microcapsules was confirmed by a comparison between the volatile compounds embedded in TTO-β-CD microcapsules and those of TTO using gas chromatography-mass spectrometry (GC–MS). The volatile compounds embedded in the TTO-β-CD microcapsules were extracted as follows: 0.20 g TTO-*β-CD* microcapsules were extracted with 40 mL ethanol (99.5%) in a 50 mL centrifuge tube using the vortex mixer at 3 000 r/min for 10 min, followed by a few steps of centrifugation at 1 700 g for 10 min and sedimentation in the dark at 23 °C for 12 h. After that, the supernatant was filtered using a syringe filter with a pore size of 0.22 μm and 2 mL of the filtrate was adjusted to 30 mL with ethanol (99.5%). Finally, 2 μL of resulting solution (referred to as "ethanol extract of TTO-β-CD microcapsules") was injected into a GC–MS-QP2010Plus (Shimadzu, Japan) with an AOC-20i+s autosampler and the separation was achieved on an Rtx-5MS column (30 m × 0.25 μm, 0.25 μm in film thickness). The TTO sample was diluted 3×10^4 times with ethanol (99.5%) before injection to detect volatile compounds. The oven temperature of GC was programmed as follows: the temperature was initially set to 60 °C for 2 min, then increased to 125 °C at a rate of 5 °C/min and maintained for 2 min, and finally to 160 °C at 10 °C/min and maintained for 2 min. The injector temperature was 230 °C, and the flow rate of carrier helium gas was 1 mL/min with a split ratio of 10:1. The mass spectrometer was operated in the electron impact mode at 70 eV, and mass spectra were acquired using a scan mode with a mass scan range of 35–400 m/z. The temperatures of the ion source and interface were 200 and 240 °C, respectively. The solvent delay was set to 4 min. Identification of the volatile compounds was based on the comparison of their mass spectra with those of National Institute Standard and Technology version-05 and 05 s library data inserted in the GC–MS system.

Molecular interactions of TTO-β-CD microcapsules between the TTO and β-CD were confirmed via a Fourier transform infrared spectroscopy (FT-IR, FT/IR-6800, JASCO, Japan). The FT-IR spectra were collected between 4 000 and 400 cm^{-1} at a resolution of 4 cm^{-1} with averaging from 16 scans. The TTO was pasted on a potassium bromide (KBr) plate, whereas plain β-CD and TTO-β-CD microcapsules were ground with KBr powders (~50 mg dry KBr added per 1 mg plain β-CD or TTO-β-CD microcapsules) followed by pressing into a 1 mm thick pellet. Raw data of FT-IR spectra were smoothed, and the baseline was corrected via a built-in software of the spectrophotometer.

A simple growth inhibition test, using *B. subtilis* as the object microorganism, was used to assess the antibacterial activity of TTO-β-CD microcapsules and also used to confirm the formation because the fabricated microcapsules are supposed to present a certain degree of inhibitory effect if the TTO was well embedded within the hollow cavities of β-CD. For the growth inhibition assessment of TTO, a disk diffusion method was conducted as follows: 15 mL sterilized tryptic soy agar (TSA) was poured into a Petri dish (Greiner Bio-One International GmbH, Austria) with a diameter of 96 mm. After the solidification of TSA, 20 μL of 1.5×10^8 CFU/mL *B. subtilis* inoculum was inoculated into the TSA Petri dish and spread out evenly using a wire loop. A sterilized paper disk (Advantec, Toyo Roshi Kaisha, Ltd., Japan) with a diameter of 8 mm was dispensed over the surface of the TSA Petri dish. After that, 20 μL of pure TTO was added to the paper disk. In addition, a blank paper disk with 20 μL of physiological saline added was set as a control. Finally, the inoculated TSA Petri dish was sealed with a Riken wrap and incubated at 37 °C for 24 h. For the growth inhibition assessment of β-CD-MEOs microcapsules, the experimental details were as follows: 15 mL TSA was poured into a Petri dish. After the solidification of TSA, a small hole in the middle of the TSA Petri dish was dug out using a sterile knife, followed by an injection of 20 μL 1.5×10^8 CFU/mL *B. subtilis* inoculum into this hole. The 0.03 g TTO-β-CD microcapsules (plain β-CD was set as a control) were placed equidistantly on both sides of the small hole, respectively. Finally, the inoculated TSA Petri dish was sealed with the Riken wrap and incubated at 37 °C for 24 h. All operations above were carried out in a clean bench (CCV-811, Hitachi, Japan).

The water contact angle using a sessile drop technique was used to evaluate the hydrophilicity of the TTO-β-CD microcapsules. The samples were prepared according to the methodology described by Sarkar and Mahapatra (2014) with a few modifications. Briefly,

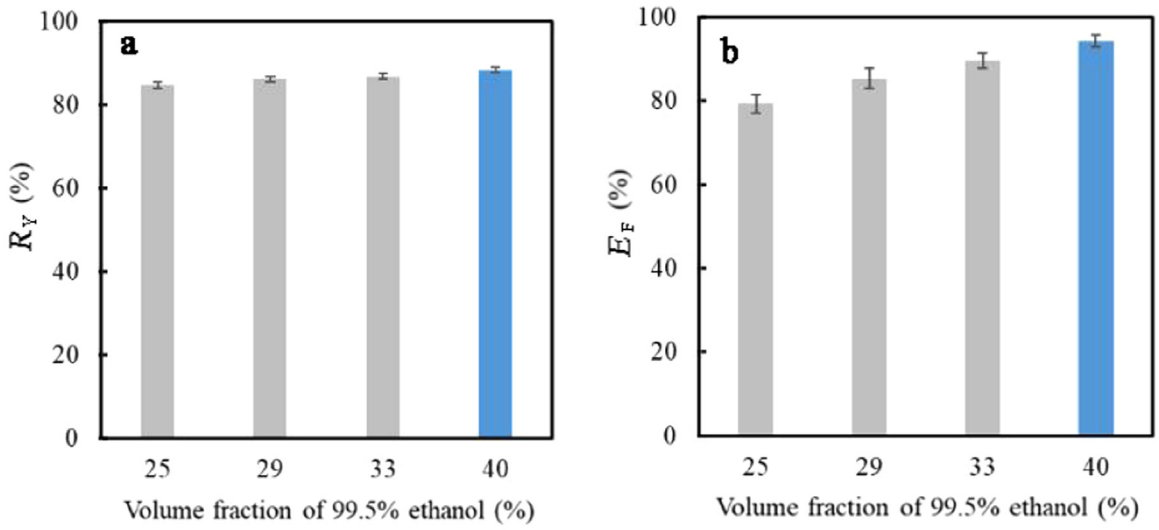

Fig. 1. Effect of various volume fractions of 99.5% ethanol on co-solvent on recovery yield (R_Y) (a) and embedding fraction (E_F) (b).

~0.2 g TTO-β-CD microcapsules were spread uniformly on the surface of a glass slide and pressed via a thermal-press machine (HC300–01, AS ONE Corporation, Japan) at 30 MPa and room temperature for 30 s. After pressing, the slide was flushed slightly with air using a mini rubber blower to remove the free TTO-β-CD microcapsules. The water contact angle was measured with an automatic Contact Angle Meters DropMaster (DMs-401, Kyowa Interface Science, Japan). Milli-Q water with a volume of 2 μL was deposited on the surface using a high-precision injector. After equilibration, the measurement was conducted with a $\theta/2$ method, and the images were photographed using a high-speed video camera installed on the equipment system.

3. Results and discussion

3.1. Encapsulation efficiency analysis

Microencapsulation using β-CD with the ability to embed hydrophobic TTO into its inner cavity was applied to avert the drawbacks of TTO caused by its instability in natural ambient conditions. Two parameters: R_Y and E_F, were used as indicators for the evaluation of encapsulation efficiency. Fig. 1 shows the effect of varied volume fractions of 99.5% ethanol in the co-solvent on R_Y and E_F. Overall, the results showed that the R_Y and E_F values were higher than 84% and 79%, respectively. Anaya-Castro et al. (2017) reported that all the R_Y values obtained at different mass ratios of oregano or clove oil to β-CD via the co-precipitation method were above 88%, whereas the values of E_F merely ranged from 30% to 78%. The authors explained that the large variation in E_F was presented when the mass ratio of EOs to β-CD was varied. Compared to our previous results (Kong et al., 2022a), the remarkable increase in E_F in this study was partially derived from the optimization of the ratio of EOs to β-CD, which was reduced from 1:5 to 1:9 as also suggested by Wen et al. (2016) and Ma et al. (2018). The reduction of TTO usage not only substantially improved the E_F but also lowered the cost, given the capacity limit of β-CD for microencapsulation. In the present study, it is conceivable that the high E_F also resulted from some adjustments, such as an adequate barrier to illumination and a low co-precipitation temperature (−2 ˚C), that have been overlooked by previous researchers. The former minimized the impact of illumination on the degradation of TTO bioactive compounds during the stirring and drying processes since they are extremely unstable even under the ambient environment; the latter promoted the simplicity of co-precipitation. Moreover, based on previous reports, an oven-dry process at a relatively high temperature (e.g., 50–60 ˚C) or freeze-drying was generally applied for the moist microcapsules recovered from a suction filtration (Munhuweyi et al., 2018; Gao et al., 2020; Hogenbom et al., 2021; Castro et al., 2022). Nevertheless, these steps were avoided in this study to prevent a predicted loss of bioactive compounds out of TTO along with a heating or a high vacuum process. Meanwhile, a rinsing process with a sufficient amount (40 mL) of 60% ethanol at the end of filtration readily dried the microcapsules and drying in a desiccator at 23 ˚C for 24 h was more adequate to attain an equilibrium, as was demonstrated by a previous test.

Interestingly, a decline in encapsulation efficiency was presented as the proportion of ethanol in the co-solvent system decreased. It is worth noting that the addition of ethanol to the co-solvent not only increased the solubility of β-CD (only ~1.5 g β-CD was successfully dissolved in 50 mL water as described in Section 2.2), but also assisted in dispersing hydrophobic TTO. It has been revealed that the substitution of high enthalpy molecules in the inner cavities of β-CD by bioactive compounds is one of the predominant driving forces for microencapsulation (Astray et al., 2009). It is also stated that ethanol molecules are initially entrapped into the β-CD molecule and act as the higher enthalpy molecules, followed by a replacement with the bioactive compounds, as the latter has a superior affinity towards the hydrophobic cavities (Shrestha et al., 2017). On the one hand, the higher proportion (40%) of ethanol in this study allowed for a rapid addition of TTO to the solvent system rather than a drop-by-drop addition which was constantly applied

and reported (Wen et al., 2016; Ning and Yue, 2019). It is convincing that a drop-by-drop addition not only greatly complicates the operation but also is probably reckoned as a non-negligible barrier to large-scale production. On the other hand, it will induce co-precipitation when the solubility of microcapsules becomes lower with a higher volume fraction of ethanol. However, it is required that water comprises the majority of the co-solvent system, as 3 g β-CD failed to dissolve completely in a co-solvent when the volume fraction of 99.5% ethanol was 50% (as described in Section 2.2). Hence, the effect of the volume ratios of distilled water to 99.5% ethanol in this study was investigated in a range from 1.5 to 3, which is firstly reported to the best of our knowledge. Apparently, as shown in Fig. 1, when the volume fraction of 99.5% ethanol in the co-solvent was 40%, both R_Y and E_F exhibited the highest values, which were (88.3 ± 0.6)% and (94.3 ± 1.4)% (mean ± standard deviation, $n = 3$), respectively.

Most previous studies primarily focused on two solvent systems for the method of co-precipitation: one was (especially saturated) water solution (Yue et al., 2020), in which the added EOs were probably pre-dissolved in a small amount of ethanol (Dias Antunes et al., 2017); another one was a co-solvent of water and ethanol with a volume ratio of 2, constantly used since this condition was initially introduced by Reineccius and Risch (1986). In the study of Cui et al. (2018), TTO was encapsulated with β-CD in a water solution with a maximum EF value of 73.2%, which was significantly lower than the value in this study. Wang et al. (2011) obtained a relatively high E_F value of 90.3% when a co-solvent of water and ethanol with a volume ratio of 2 was used for the microencapsulation of garlic oil. However, as for R_Y, a much lower value of 78.2% was reported compared with the value of 86.8% in this study. A Box-Behnken design of a similar study (Ma et al., 2018) on the microencapsulation of clove oil with β-CD yielded the best values of 75.5% for R_Y and 64.6% for E_F, although those were not obtained simultaneously under the same condition. Even after the establishment of three-dimensional response surface plots and curves, maximum R_Y and E_F values anticipated under the same condition were merely 64.8% and 64.9%, respectively. Herrera et al. (2019), who prepared microcapsules of two bioactive compounds with different chemical structures, suggested that there might be a statistical distinction of E_F when the chemical structures of bioactive compounds vary. However, the encapsulation efficiency of EOs (a mixture of a variety of bioactive compounds) obtained in this study surpassed any value reported ever in previous studies, according to our knowledge.

Loading ratio (Fig. S4) is another factor that was frequently introduced to evaluate the encapsulation efficiency of microencapsulation (Kfoury et al., 2016; Anaya-Castro et al., 2017; Jiang et al., 2021a; Lin et al., 2022). It was reported that the theoretically maximum ratio of loading EOs into β-CD ranged from 8% to 12% (w) (Wen et al., 2016; Cui et al., 2018). In our study, the loading ratio of TTO was above 9% even when the volume fractions of 99.5% ethanol in the co-solvent was 25%, which was significantly higher than the value of ~6% obtained by Cui et al. (2018). This was primarily owing to the optimization of the preparation procedure as described above. In addition, when the volume fraction of 99.5% ethanol was 40%, the loading ratio reached (10.6 ± 0.1)%, which was extremely close to the maximum extent, indicating that it was easier for the bioactive components of TTO to enter into cavities of β-CD when the ethanol concentration was higher.

Time and energy are other critical aspects for evaluating encapsulation efficiency since they may have a considerable impact on large-scale production. The magnetic stirring method is a commonly used method for microencapsulation and is reported to take a considerable amount of time (Zhu et al., 2019). Jiang et al. (2021b) optimized the microencapsulation method from the magnetic stirring to an ultrasonic treatment at 120 W for 70 min and attained a higher encapsulation efficiency of TTO microcapsules; however, it was still lower than the value obtained in this study in which only 2 h of magnetic stirring was sufficient to reach a satisfactory result. We likewise studied the effect of two microencapsulation methods on encapsulation efficiency when the volume fraction of ethanol (99.5%) was 40% (Fig. S5): stirring at 45 °C described in Section 2.2 for 120 min and stirring at 45 °C for 100 min followed by ultrasonication at 40 kHz and 45 °C for 20 min in an ultrasonic bath (MCD-27, AS ONE Corporation, Japan). It was observed that R_Y and E_F decreased to varying degrees when stirring was replaced with ultrasonication for the last 20 min. The reduction of R_Y and E_F was not anticipated because the ultrasonication consumed more energy and contrarily assisted in the release of bioactive compounds that had already entered the cavities of β-CD, resembling an extraction step, as opposed to aiding the bioactive compounds to be embedded.

In summary, taking into account the values of R_Y and E_F, as well as the time and energy consumption, super-high encapsulation efficiency and an economical preparation procedure were validated.

3.2. The SEM analysis

Since the morphological structure was significantly similar when the microcapsules prepared at varied volume fractions of 99.5% ethanol in the co-solvent (Fig. S6), only the TTO-β-CD microcapsules prepared at the volume fraction of 40% were chosen for SEM and subsequent analysis. Fig. 2 shows the SEM images of plain *β-CD* and TTO-β-CD microcapsules. Plain β-CD, as purchased, appeared as irregularly homogeneous massive or lamellar plates with well-grown crystals of varying sizes, and there were distinct small particles and some fractures or striations that generated on the surfaces of crystals, in consistency with the results reported by Kotronia et al. (2017) and Barbieri et al. (2018). After the microencapsulation, it was observed that TTO-β-CD microcapsules were shaped rhomboidal with a much smaller size compared with the plain β-CD and notably tended to an agglomeration. However, no visible fractures or striations occurred, signifying adequate protection of bioactive compounds elucidated by Anaya-Castro et al. (2017). Lin et al. (2022) also studied the inclusion complexes of β-CD with *p*-anisaldehyde and reported that the complexes presented an apparent reduction in size and rhomboidal crystals. The SEM images implied that the morphology and crystal structure of the TTO-β-CD microcapsules were obviously different from those of plain β-CD. In our previous study (Kong et al., 2022b), the morphology of a blank sample of *β-CD* microcapsules without the addition of any EOs was inconsistent with that of plain β-CD and appeared to be more granular; however, only a deviation on crystal orientation rather than the structure was detected by XRD patterns, indicating that the TTO had a substantial impact on the crystal structure which would be affirmed by the following XRD analysis.

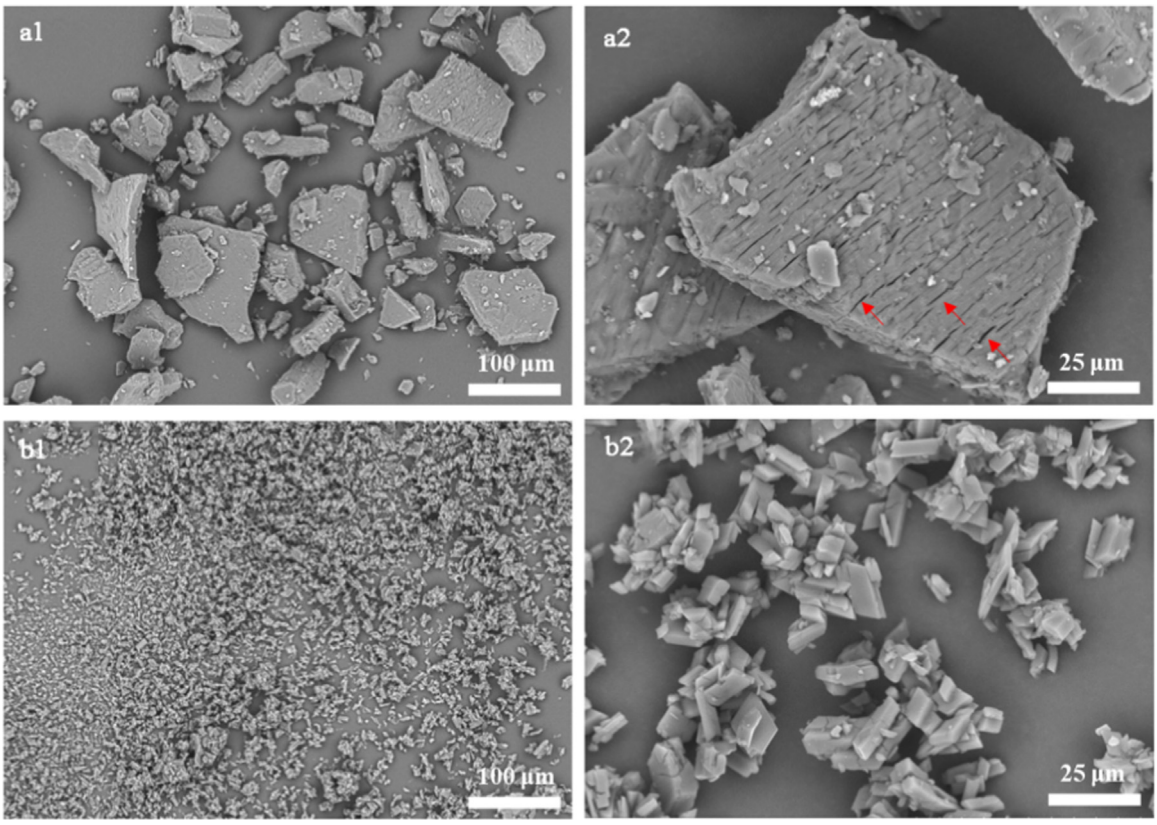

Fig. 2. Scanning electron microscope (SEM) images of plain β-cyclodextrin (β-CD) (a1, a2) and tea tree oil (TTO)-β-CD microcapsules (b1, b2).

3.3. The XRD analysis

The XRD is a useful method for the confirmation of crystalline states. Fig. 3 shows the XRD patterns of plain β-CD and TTO-β-CD microcapsules. Evidently, the XRD diffraction pattern of TTO-β-CD microcapsules was distinct from that of plain β-CD. It has been commonly stated that the crystal structures of β-CD are generally divided into two categories: cage and channel types (Fig. S7) (Shrestha et al., 2017; Poulson et al., 2021). It is also reported that plain β-CD is a crystalline material with cage type structure where each cavity is blocked by neighboring β-CD molecules, and hence the cavity is not available to form a microcapsule with the core molecules. However, the crystal structure can be transformed into channel type structure (head-to-head or head-to-tail orientation) where β-CD molecules are stacked on top of each other to form long cylindrical channels by a re-precipitation process in which β-CD are dissolved in a solvent and precipitated at a low temperature (Celebioglu et al., 2017; Shrestha et al., 2017). The diffraction angle 2θ of the TTO-β-CD microcapsules presented five major peaks at 7.2°, 9.9°, 12.0°, 17.5°, and 18.7°, whereas the plain β-CD exhibited sharp peaks at 10.6°, 12.5°, 14.7°, 17.7°, 18.7°, and 20.8° According to the reports of Li et al. (2013) and Ogata et al. (2020), the large variations in these characteristic peaks correspond to the structural transition of β-CD from cage type to channel type before and after microencapsulation. Moreover, changes in the crystal structure also reflected either the disappearance of the peaks at 4.5° and 8.9° or the appearance of a new peak at 7.2°, in accordance with the result of Abarca et al. (2016), who also described these changes could be associated with some changes in the molecular organization of β-CD from cage type to channel type. Additionally, Celebioglu et al. (2017) mentioned that the crystal structure of the channel type had a smaller and more regular shape, agreeing with the SEM observations.

3.4. The GC–MS analysis

Identification of the volatile bioactive compounds in TTO and TTO-β-CD microcapsules was accomplished via a GC–MS analysis. Fig. 4 shows the total ion chromatograms of TTO and ethanol extract of TTO-β-CD microcapsules. Fig. 5 shows the nine typical compounds labelled from “a” to “i” in Fig. 4. Visually, the total ion chromatograms of ethanol extract of TTO-β-CD microcapsules were almost identical to that of TTO. Interestingly, a slight difference in the intensity of some compounds was present during the retention time from 14 to 22 min, which could be explained by the fact that the compounds with longer molecular chains (e.g., 1,3-di-*tert*-butylbenzene and 2,4-di-*tert*-butylphenol) or larger molecular weights (e.g., tetradecane) struggled to be embedded during the microencapsulation. The compounds detected during the retention time from 6 to 14 min, corresponding to the oven temperature

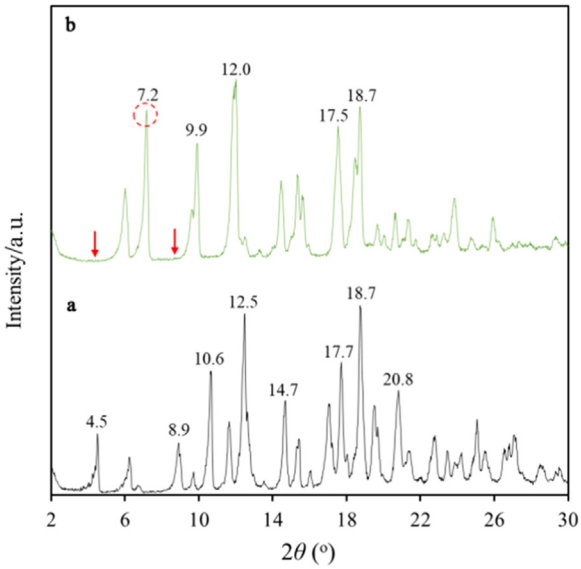

Fig. 3. The X-ray diffractometer (XRD) patterns of plain β-CD (a) and TTO-β-CD microcapsules (b).

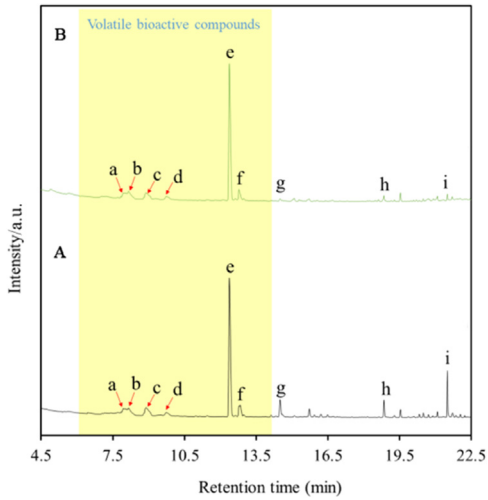

Fig. 4. Total ion chromatograms of TTO (A) and ethanol extract of TTO-β-CD microcapsules (B).

of GC from 80 to 120 ˚C, were regarded as volatile bioactive compounds. Among them, terpinen-4-ol was the principal constituent, with a minimum content of 30% reported by Yadav et al. (2017) and Shrestha et al. (2017). Some other major bioactive compounds, such as γ-terpinene, 1,8-cineole, and terpinolene, were also detected in the ethanol extract of TTO-β-CD microcapsules, indicating that the TTO was well embedded within the hollow cavities of β-CD via the co-precipitation method.

3.5. The FT-IR analysis

The FT-IR technique is commonly used to estimate the interaction between β-CD and core molecules in terms of the peak shape, position, and intensity (Abarca et al., 2016; Kotronia et al., 2017; Wang et al., 2011). Fig. 6 shows the FT-IR spectra of TTO, plain β-CD, and TTO-β-CD microcapsules. Typically, TTO exhibited prominent peaks at 3 428 cm^{-1} (for stretching vibrations of O–H) and 2 961–2 928 cm^{-1} (for symmetrical and asymmetrical stretching vibrations of $–CH_3$ and $–CH_2–$). The weak absorption peaks presented from 1 800–1 600 cm^{-1} were exhibited by the stretching vibrations of C=C from terpenes. The two strong bands located at ~1 500 and 1 380 cm^{-1} arose from the aromatic C=C and scissoring vibrations of $–CH_2–$ and $–CH_3$, respectively (Cui et al., 2018; Gallart-Mateu et al., 2018), while the medium peaks located at 1 150– ~850 cm^{-1} were derived from the stretching vibration of the C–O bond in terpineol (Lin et al., 2018). The medium peaks located at ~900 cm^{-1} were derived from the symmetrical stretching vibrations of C–O–C from 1,8-cineole. The weak peak located between 860 and 800 cm^{-1} (for out-of-plane bending vibrations of

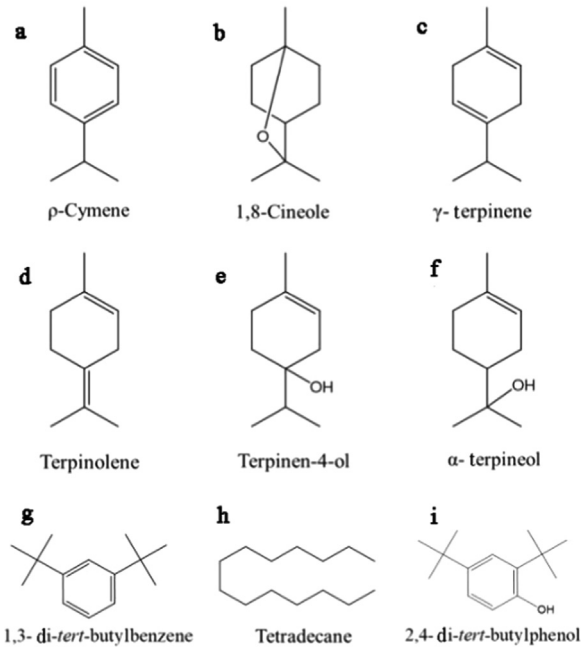

Fig. 5. Nine typical compounds identified from TTO. The a–i represent the typical compounds labelled from "a" to "i" in Fig. 4.

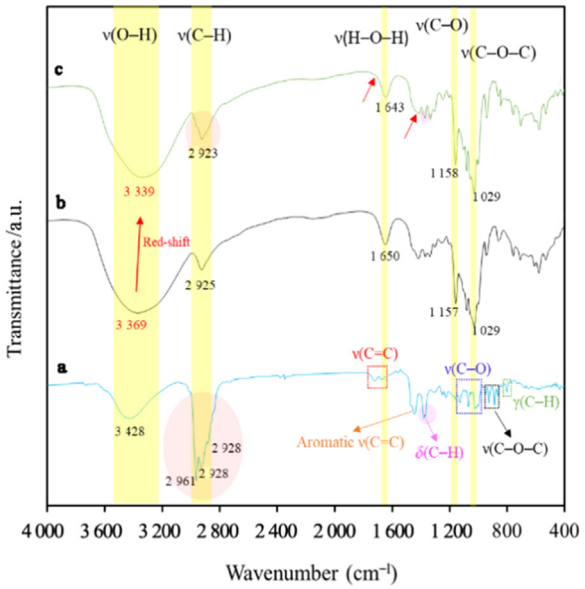

Fig. 6. Fourier transform infrared (FT-IR) spectra of TTO (a), plain β-CD (b), and TTO-β-CD microcapsules (c).

C–H) was probably linked to the para-substitution of benzene primarily from the *p*-cymene of TTO. The main absorption bands of plain β-CD were observed at 3 369, 2 925, 1 650, 1 157, and 1 029 cm^{-1}, corresponding to the symmetrical and asymmetrical stretching vibrations of O–H, stretching vibrations of C–H, bending of H–O–H, stretching vibrations of C–O, and symmetrical and asymmetrical stretching vibrations of C–O–C, respectively (Abarca et al., 2016; Wang et al., 2011). Noticeably, the spectra of TTO-β-CD microcapsules were practically dominated by the bands of plain β-CD. The highly intense absorption peaks of TTO located at 2 961–2 928 cm^{-1} were remarkably weakened in the spectra of TTO-β-CD microcapsules, as well as the partially decreased intensity of the peak located ~1 380 cm^{-1}. Furthermore, the aromatic C=C peaks were completely concealed by the β-CD, in line with the findings of Wen et al. (2016) and Menezes et al. (2012), who considered these changes to be related to the successful formation of microcapsules. It is also worth noting that the position of the O–H absorption peak of TTO-β-CD microcapsules shifted towards lower frequencies (red-shift) with respect to the plain β-CD, elucidated by Munhuweyi et al. (2018) that this shift indicated an interaction

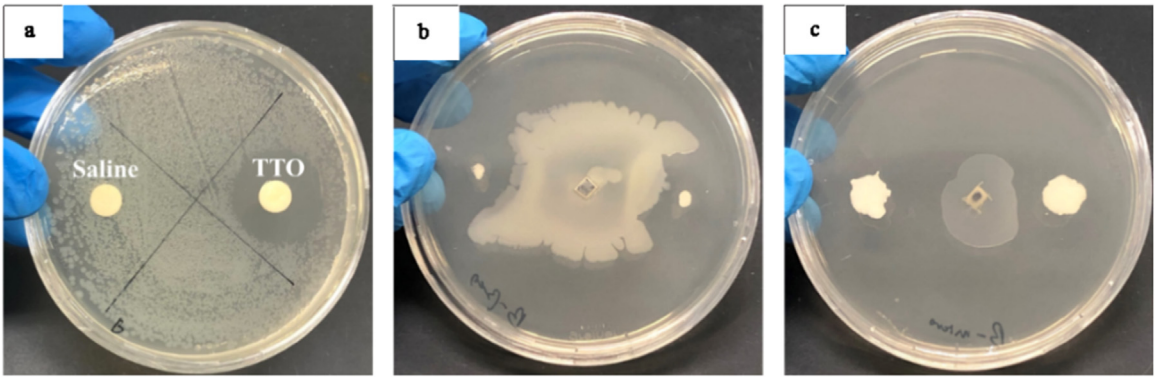

Fig. 7. Growth inhibitory effects of pure TTO (a), plain β-CD (b), and TTO-β-CD microcapsules (c) against *Bacillus subtilis* after incubation at 37 °C for 24 h.

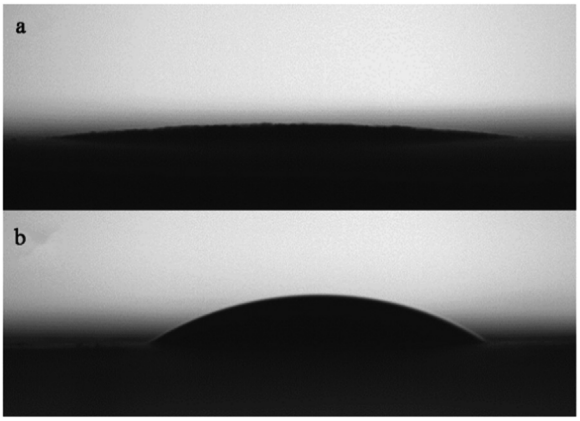

Fig. 8. Water contact angles of plain β-CD (a) and TTO-β-CD microcapsules (b).

had occurred between the bioactive compounds and β-CD via hydrogen bonding, indicative of the successful microencapsulation just as confirmed by GC–MS analysis.

3.6. Antibacterial activity of TTO-β-CD microcapsules

To investigate the antibacterial activity of the fabricated TTO-β-CD microcapsules, a simple growth inhibition test using *B. subtilis* as the study object was performed, and the results were present in Fig. 7. Fig. 7a shows the growth inhibitory effect of pure TTO against the *B. subtilis*. Apparently, a huge inhibitory zone was present after the incubation for 24 h, demonstrating its excellent antibacterial activity, as also reported by Yadav et al. (2017). Fig. 7b–c show the growth status of *B. subtilis* in TSA medium with the addition of plain β-CD and TTO-β-CD microcapsules after the incubation for 24 h. Plain β-CD resulted in the rapid growth and breeding of *B. subtilis* due to the fact that β-CD is a polysaccharide that can provide a carbohydrate source and act as a nutrient to the *B. subtilis*. On the contrary, the addition of microcapsules containing TTO showed a potent growth inhibitory ability which exhibited a satisfactory antibacterial activity of the fabricated microcapsules. Furthermore, this fact indirectly revealed the TTO was successfully encapsulated within hollow cavities of β-CD, as estimated from the GC–MS and FT-IR analysis.

3.7. Hydrophilicity of TTO-β-CD microcapsules

The microencapsulation of EOs with β-CD not only reduces its volatility and enables a sustained release but also endows it simpler to incorporate with other hydrophilic substances owing to the hydrophilic outer surface of the β-CD, resulting in a wide range of potential applications in numerous fields (Wang et al., 2011). The hydrophilicity of the fabricated TTO-β-CD microcapsules was ascertained by measurement of the water contact angle. Fig. 8 shows the images of the contact angle of plain β-CD and TTO-β-CD microcapsules, which were calculated to be $(7.5 \pm 0.4)^\circ$ and $(31.3 \pm 2.3)^\circ$ (mean $\pm$ standard deviation, $n = 3$), respectively. Because of the water solubility of β-CD, its contact angle was extremely low, in line with the results reported by Xi et al. (2018) and Hu et al. (2020). After the introduction of TTO to the hollow cavities of the β-CD molecule, the contact angle of TTO-β-CD microcapsules increased to a certain degree, which could be attributed to the distribution of hydrophobic compounds of TTO inside the microcapsules. However, it was much lower than 90°, proving good hydrophilicity of the fabricated microcapsules.

4. Conclusions

This study prepared TTO-β-CD microcapsules using a co-precipitation method and focused on the impact of the volume fraction of ethanol in the co-solvent on encapsulation efficiency. The encapsulation efficiency analysis revealed that the recovery yield (R_Y) and TTO embedding fraction (E_F) increased when the volume fraction (ranging from 25% to 40%) of ethanol in the co-solvent was higher. Especially when the volume fraction of ethanol in the co-solvent was 40%, R_Y and E_F were as high as 88.3% and 94.3%, respectively, which surpassed any value reported ever in previous studies, according to our knowledge. Moreover, considering the time and energy consumption, an economical preparation procedure to make large-scale production feasible was established. The SEM and XRD results showed that the crystal structure appeared to be distinctively different before and after the microencapsulation procedure. The results of GC–MS and FT-IR confirmed that the TTO was successfully embedded within hollow cavities of β-CD. The antibacterial activity of the TTO-β-CD microcapsule was proved by a simple growth inhibition test using *B. subtilis* as the object microorganism. The water contact angle confirmed the hydrophilicity of microcapsules, allowing it easier to integrate them with hydrophilic biodegradable materials for versatile applications. Further work on the release properties of the TTO from the microcapsules under varied environmental circumstances, such as humidity and temperature, can be considered.

Declaration of Competing Interest

There are no conflicts to declare.

Acknowledgements

We would like to thank the Open Facility centre, the University of Tsukuba for allowing us to use its facilities. We also thank the operating budget from the University of Tsukuba for the support of this study. P. K. would like to thank the JST SPRING (Grant No.: JPMJSP2124) for the support of his life and this study. P. K. also thanks Prof. Naoki Takaya for the free use of his laboratory equipment.

Supplementary materials

Supplementary material associated with this article can be found, in the online version, at doi:10.1016/j.jobab.2023.03.004.

References

Abarca, R.L., Rodríguez, F.J., Guarda, A., Galotto, M.J., Bruna, J.E., 2016. Characterization of beta-cyclodextrin inclusion complexes containing an essential oil component. Food Chem. 196, 968–975.

Anaya-Castro, M.A., Ayala-Zavala, J.F., Muñoz-Castellanos, L., Hernández-Ochoa, L., Peydecastaing, J., Durrieu, V., 2017. β-Cyclodextrin inclusion complexes containing clove (*Eugenia caryophyllata*) and Mexican oregano (*Lippia berlandieri*) essential oils: preparation, physicochemical and antimicrobial characterization. Food Packag. Shelf Life 14, 96–101.

Astray, G., Gonzalez-Barreiro, C., Mejuto, J.C., Rial-Otero, R., Simal-Gándara, J., 2009. A review on the use of cyclodextrins in foods. Food Hydrocoll. 23, 1631–1640.

Aytac, Z., Kusku, S.I., Durgun, E., Uyar, T., 2016. Quercetin/β-cyclodextrin inclusion complex embedded nanofibres: slow release and high solubility. Food Chem. 197, 864–871.

Barbieri, N., Sanchez-Contreras, A., Canto, A., Cauich-Rodriguez, J.V., Vargas-Coronado, R., Calvo-Irabien, L.M., 2018. Effect of cyclodextrins and Mexican oregano (*Lippia graveolens* Kunth) chemotypes on the microencapsulation of essential oil. Ind. Crops Prod. 121, 114–123.

Castro, J.C., Pante, G.C., de Souza, D.S., Pires, T.Y., Miyoshi, J.H., Garcia, F.P., Nakamura, C.V., Mulati, A.C.N., Mossini, S.A.G., Machinski Jr, M., Matioli, G., 2022. Molecular inclusion of *Cymbopogon martinii* essential oil with β-cyclodextrin as a strategy to stabilize and increase its bioactivity. Food Hydrocoll. Health 2, 100066.

Celebioglu, A., Ipek, S., Durgun, E., Uyar, T., 2017. Selective and efficient removal of volatile organic compounds by channel-type gamma-cyclodextrin assembly through inclusion complexation. Ind. Eng. Chem. Res. 56, 7345–7354.

Cui, H.Y., Bai, M., Lin, L., 2018. Plasma-treated poly(ethylene oxide) nanofibers containing tea tree oil/beta-cyclodextrin inclusion complex for antibacterial packaging. Carbohydr. Polym. 179, 360–369.

de Almeida Magalhães, T.S.S., de Oliveira Macedo, P.C., Kawashima Pacheco, S.Y., Silva, S.S.D., Barbosa, E.G., Pereira, R.R., Costa, R.M.R., Silva Junior, J.O.C., da Silva Ferreira, M.A., de Almeida, J.C., Rolim Neto, P.J., Converti, A., de Lima, Á.A.N., 2020. Development and evaluation of antimicrobial and modulatory activity of inclusion complex of *Euterpe oleracea* mart oil and β-cyclodextrin or HP-β-cyclodextrin. Int. J. Mol. Sci. 21, 942.

Dias Antunes, M., da Silva Dannenberg, G., Fiorentini, Â.M., Pinto, V.Z., Lim, L.T., da Rosa Zavareze, E., Dias, A.R.G., 2017. Antimicrobial electrospun ultrafine fibers from zein containing eucalyptus essential oil/cyclodextrin inclusion complex. Int. J. Biol. Macromol. 104, 874–882.

Gallart-Mateu, D., Largo-Arango, C.D., Larkman, T., Garrigues, S., de la Guardia, M., 2018. Fast authentication of tea tree oil through spectroscopy. Talanta 189, 404–410.

Gao, S., Jiang, J.Y., Li, X.M., Liu, Y.Y., Zhao, L.X., Fu, Y., Ye, F., 2020. Enhanced physicochemical properties and herbicidal activity of an environment-friendly clathrate formed by β-cyclodextrin and herbicide cyanazine. J. Mol. Liq. 305, 112858.

Gao, S., Liu, Y.Y., Jiang, J.Y., Li, X.M., Ye, F., Fu, Y., Zhao, L.X., 2021. Thiram/hydroxypropyl-β-cyclodextrin inclusion complex electrospun nanofibers for a fast dissolving water-based drug delivery system. Colloids Surf. B 201, 111625.

Herrera, A., Rodríguez, F.J., Bruna, J.E., Abarca, R.L., Galotto, M.J., Guarda, A., Mascayano, C., Sandoval-Yáñez, C., Padula, M., Felipe, F.R.S., 2019. Antifungal and physicochemical properties of inclusion complexes based on β-cyclodextrin and essential oil derivatives. Food Res. Int. 121, 127–135.

Hogenbom, J., Jones, A., Wang, H.V., Pickett, L.J., Faraone, N., 2021. Synthesis and characterization of β-cyclodextrin-essential oil inclusion complexes for tick repellent development. Polymers 13, 1892.

Hu, Y., Qiu, C., Jin, Z.Y., Qin, Y., Zhan, C., Xu, X.M., Wang, J.P., 2020. Pickering emulsions with enhanced storage stabilities by using hybrid β-cyclodextrin/short linear glucan nanoparticles as stabilizers. Carbohydr. Polym. 229, 115418.

Jiang, L.W., Wang, P.Z., Kou, L.H., Wei, H.Y., Ren, L.L., Zhou, J., 2021a. Preparation and physicochemical properties of catechin/β-cyclodextrin inclusion complex nanoparticles. Food Biophys. 16, 317–324.

Jiang, S., Zhao, T.T., Wei, Y.Y., Cao, Z.D., Xu, Y.Y., Wei, J.Y., Xu, F., Wang, H.F., Shao, X.F., 2021b. Preparation and characterization of tea tree oil/hydroxypropyl-β-cyclodextrin inclusion complex and its application to control brown rot in peach fruit. Food Hydrocoll. 121, 107037.

Ju, J., Chen, X.Q., Xie, Y.F., Yu, H., Guo, Y.H., Cheng, Y.L., Qian, H., Yao, W.R., 2019. Application of essential oil as a sustained release preparation in food packaging. Trends Food Sci. Technol. 92, 22–32.

Kfoury, M., Auezova, L., Greige-Gerges, H., Larsen, K.L., Fourmentin, S., 2016. Release studies of *trans*-anethole from β-cyclodextrin solid inclusion complexes by Multiple Headspace Extraction. Carbohydr. Polym. 151, 1245–1250.
Kong, P.F., Abe, J.P., Enomae, T., 2022a. Preparation of antimicrobial 6-cyclodextrin microcapsules containing a mixture of three essential oils as an eco-friendly additive for active food packaging paper. J. Tappi J. 76, 656–662.
Kong, P.F., Abe, J.P., Nakagawa-izumi, A., Kajiyama, M., Enomae, T., 2022b. Preparation of an eco-friendly antibacterial agent for food packaging containing *Houttuynia cordata* Thunb. extract. RSC Adv 12, 16141–16152.
Kotronia, M., Kavetsou, E., Loupassaki, S., Kikionis, S., Vouyiouka, S., Detsi, A., 2017. Encapsulation of oregano (*Origanum onites* L.) essential oil in β-cyclodextrin (β-CD): synthesis and characterization of the inclusion complexes. Bioengineering 4, 74.
Lam, N.S., Long, X.X., Su, X.Z., Lu, F.L., 2020. *Melaleuca alternifolia* (tea tree) oil and its monoterpene constituents in treating protozoan and helminthic infections. Biomed. Pharmacother. 130, 110624.
Li, P.Y., Song, J., Ni, X.M., Guo, Q., Wen, H., Zhou, Q.Y., Shen, Y.N., Huang, Y.J., Qiu, P.X., Lin, S.Z., Hu, H.Y., 2016. Comparison in toxicity and solubilizing capacity of hydroxypropyl-β-cyclodextrin with different degree of substitution. Int. J. Pharm. 513, 347–356.
Li, S.Y., Xing, P.Y., Hou, Y.H., Yang, J.S., Yang, X.Z., Wang, B., Hao, A.Y., 2013. Formation of a sheet-like hydrogel from vesicles *via* precipitates based on an ionic liquid-based surfactant and β-cyclodextrin. J. Mol. Liq. 188, 74–80.
Lin, G.Q., Chen, H.Y., Zhou, H.J., Zhou, X.H., Xu, H., 2018. Preparation of tea tree oil/poly(styrene-butyl methacrylate) microspheres with sustained release and anti-bacterial properties. Materials 11, 710.
Lin, Y., Huang, R., Sun, X.X., Yu, X., Xiao, Y., Wang, L., Hu, W.Z., Zhong, T., 2022. The *p*-Anisaldehyde/β-cyclodextrin inclusion complexes as a sustained release agent: characterization, storage stability, antibacterial and antioxidant activity. Food Control 132, 108561.
Lis, M.J., García Carmona, Ó., García Carmona, C., Maestá Bezerra, F., 2018. Inclusion complexes of *Citronella* oil with β-cyclodextrin for controlled release in biofunctional textiles. Polymers 10, 1324.
Liu, Z.J., Ye, L., Xi, J.N., Wang, J., Feng, Z.G., 2021. Cyclodextrin polymers: structure, synthesis, and use as drug carriers. Prog. Polym. Sci. 118, 101408.
Ma, S.S., Zhao, Z.Y., Liu, P.H., 2018. Optimization of preparation process of β-cyclodextrin inclusion compound of clove essential oil and evaluation of heat stability and antioxidant activities in vitro. J. Food Meas. Charact. 12, 2057–2067.
Menezes, P.P., Serafini, M.R., Santana, B.V., Nunes, R.S., Quintans, L.J., Silva, G.F., Medeiros, I.A., Marchioro, M., Fraga, B.P., Santos, M.R.V., Araújo, A.A.S., 2012. Solid-state β-cyclodextrin complexes containing geraniol. Thermochim. Acta 548, 45–50.
Mishra, A.P., Devkota, H.P., Nigam, M., Adetunji, C.O., Srivastava, N., Saklani, S., Shukla, I., Azmi, L., Ali Shariati, M., Melo Coutinho, H.D., Mousavi Khaneghah, A., 2020. Combination of essential oils in dairy products: a review of their functions and potential benefits. LWT 133, 110116.
Munhuweyi, K., Caleb, O.J., van Reenen, A.J., Opara, U.L., 2018. Physical and antifungal properties of β-cyclodextrin microcapsules and nanofibre films containing cinnamon and oregano essential oils. LWT 87, 413–422.
Ning, J.X., Yue, S.L., 2019. Optimization of preparation conditions of eucalyptus essential oil microcapsules by response surface methodology. J. Food Process. Preserv. 43, e14188.
Ogata, Y., Inoue, Y., Ikeda, N., Murata, I., Kanamoto, I., 2020. Improvement of stability due to a *Cyclamen aldehyde*/β-cyclodextrin inclusion complex. J. Mol. Struct. 1215, 128161.
Poulson, B.G., Alsulami, Q.A., Sharfalddin, A., El Agammy, E.F., Mouffouk, F., Emwas, A.H., Jaremko, L., Jaremko, M., 2021. Cyclodextrins: structural, chemical, and physical properties, and applications. Polysaccharides 3, 1–31.
Reineccius, G.A., Risch, S.J., 1986. Encapsulation of artificial flavours by β-cyclodextrin. Perfum. Flavor. 11, 1–6.
Sadgrove, N., Jones, G., 2015. A contemporary introduction to essential oils: chemistry, bioactivity and prospects for Australian agriculture. Agriculture 5, 48–102.
Sarkar, A., Mahapatra, S., 2014. Novel hydrophobic vaterite particles for oil removal and recovery. J. Mater. Chem. A 2, 3808–3818.
Sarkic, A., Stappen, I., 2018. Essential oils and their single compounds in cosmetics—a critical review. Cosmetics 5, 11.
Sathiyaseelan, A., Saravanakumar, K., Mariadoss, A.V.A., Ramachandran, C., Hu, X.W., Oh, D.H., Wang, M.H., 2021. Chitosan-tea tree oil nanoemulsion and calcium chloride tailored edible coating increase the shelf life of fresh cut red bell pepper. Prog. Org. Coat. 151, 106010.
Sharma, S., Barkauskaite, S., Jaiswal, A.K., Jaiswal, S., 2021. Essential oils as additives in active food packaging. Food Chem 343, 128403.
Shrestha, M., Ho, T.M., Bhandari, B.R., 2017. Encapsulation of tea tree oil by amorphous beta-cyclodextrin powder. Food Chem 221, 1474–1483.
Wang, J., Cao, Y.P., Sun, B.G., Wang, C.T., 2011. Physicochemical and release characterisation of garlic oil-β-cyclodextrin inclusion complexes. Food Chem 127, 1680–1685.
Wei, Y.Q., Zhang, J., Zhou, Y., Bei, W.Y., Li, Y., Yuan, Q.P., Liang, H., 2017. Characterization of glabridin/hydroxypropyl-β-cyclodextrin inclusion complex with robust solubility and enhanced bioactivity. Carbohydr. Polym. 159, 152–160.
Wen, P., Zhu, D.H., Feng, K., Liu, F.J., Lou, W.Y., Li, N., Zong, M.H., Wu, H., 2016. Fabrication of electrospun polylactic acid nanofilm incorporating cinnamon essential oil/β-cyclodextrin inclusion complex for antimicrobial packaging. Food Chem 196, 996–1004.
Xi, Y.K., Luo, Z.G., Lu, X.X., Peng, X.C., 2018. Modulation of cyclodextrin particle amphiphilic properties to stabilize Pickering emulsion. J. Agric. Food Chem. 66, 228–237.
Yadav, E., Kumar, S., Mahant, S., Khatkar, S., Rao, R., 2017. Tea tree oil: a promising essential oil. J. Essent. Oil Res. 29, 201–213.
Yao, Y.S., Xie, Y., Hong, C., Li, G.W., Shen, H.Y., Ji, G., 2014. Development of a myricetin/hydroxypropyl-β-cyclodextrin inclusion complex: preparation, characterization, and evaluation. Carbohydr. Polym. 110, 329–337.
Yue, Q., Shao, X.F., Wei, Y.Y., Jiang, S., Xu, F., Wang, H.F., Gao, H.Y., 2020. Optimized preparation of tea tree oil complexation and their antifungal activity against *Botrytis cinerea*. Postharvest Biol. Technol. 162, 111114.
Zhang, N., Yao, L., 2019. Anxiolytic effect of essential oils and their constituents: a review. J. Agric. Food Chem. 67, 13790–13808.
Zhu, G.Y., Zhu, G.X., Xiao, Z.B., 2019. A review of the production of slow-release flavor by formation inclusion complex with cyclodextrins and their derivatives. J. Inclusion Phenom. Macrocycl. Chem 95, 17–33.